Renewable Energy 91 (2016) 442–450

Contents lists available at ScienceDirect

Renewable Energy

journal homepage: www.elsevier.com/locate/renene

Decadal variability of wave power production in the North-East Atlantic and North Sea for the M4 machine

H. Santo [a, *], P.H. Taylor [a], R. Eatock Taylor [a], P. Stansby [b]

[a] Department of Engineering Science, University of Oxford, Parks Road, Oxford OX1 3PJ, UK
[b] School of Mechanical, Aerospace and Civil Engineering, University of Manchester, Manchester M13 9PL, UK

ARTICLE INFO

Article history:
Received 1 September 2015
Received in revised form
19 January 2016
Accepted 26 January 2016
Available online 4 February 2016

Keywords:
M4 wave energy converter
Wave power variability
NAO
Correlation

ABSTRACT

We look at the variability of the power produced by the three-float M4 wave energy converter for locations in the North-East Atlantic and North Sea using the NORA10 hindcast data from 1958–2011. The aim is to investigate whether the produced power is also strongly affected by the climate variability (such as the North Atlantic Oscillations) in the winter, just as the ocean wave power resource as observed in previous studies. In this study, we demonstrate the use of proxy indices in combination with the climate indices to reconstruct a historic practical wave power climate from 1665–2005. We also conduct sensitivity studies to assess the changes in the practical wave power variability in response to perturbing the machine size, the power take-off coefficient, the response bandwidth and the power limit of the power take off. We find that the resultant temporal variation is still dominated by the climate variability. However, the overall variability important for power availability and energy supply economics is smaller than that of the ocean wave power resource because of the finite capture bandwidth of the M4 machine. The statistical methodology presented here is also potentially relevant to other wave energy converters in similar locations.

1. Introduction

The variability of the wave energy resource in the open ocean is large and spans multiple timescales. This limits our ability to predict accurately the future resource and yield from wave energy schemes. Recently, high correlations have been reported between local wave power resources and the large-scale atmospheric pressure anomalies (teleconnections). Most of the studies have focussed on the wave power variability in the North-East Atlantic, and established a positive correlation with the dominant teleconnection, the North Atlantic Oscillation (NAO), for example see [2,7–9,12].

In this paper, we assess the variability of the wave power produced by a particular device: the M4 wave energy converter in the North-East Atlantic and North Sea using hindcast data (wave model driven by carefully reconstructed weather information) from 1958–2011. The objective is to assess whether the converted or practical wave power is also strongly correlated to the NAO, just as the ocean wave power resource. A somewhat similar study was conducted by [6] for the Pelamis wave energy converter. What is different in our study is that we introduce the correlation of the practical wave power to the NAO and other significant atmospheric modes; these being the East Atlantic pattern (EA) and the Scandinavian pattern (SCA). We use these to perform a reconstruction of the practical wave power back to 1665 to assess the power characteristics of a M4 wave farm over 10 and 20 years of representative intended operational life. We note that even though the focus is on the M4 machine, the statistical methodology presented in our paper is potentially relevant to other wave energy converters.

We first present the data and the methodology to estimate the practical wave power produced by the M4 machine. We then present the performance of the practical wave power in terms of the annual value and correlate the temporal variability with the teleconnections. The last section presents a sensitivity study on the key design parameters of the M4 machine.

Previous work on the M4 wave energy converter has looked at the design and performance of the M4 machine in laboratory-scale experiments [13,14] as well as coupled hydrodynamic-structural modelling [3]. Previous work on the same hindcast data has looked at the decadal variability of the ocean wave power resource [12] and the 1 in 100 year extreme wave heights [11], as well as their correlations to the NAO and other atmospheric modes.

* Corresponding author.
E-mail address: harrif.santo@eng.ox.ac.uk (H. Santo).

http://dx.doi.org/10.1016/j.renene.2016.01.086

2. Data and methods

We consider hindcast wave data at seven locations spread out in the North-East Atlantic (points 1–4) and the North Sea (points 5–7) from 1958–2011, as shown in Fig. 1. Orkney and Cornwall (points 3 & 4) correspond to locations close to the renewable energy testing sites for EMEC and WaveHub, respectively.

We use the Norwegian 10 km Reanalysis Archive (NORA10) hindcast data developed by the Norwegian Meteorological Institute [10] using a regional High-Resolution Limited Area Model (HIRLAM) (atmospheric model) [16] and the WAM Cycle-4 (wave model) [18] hindcast covering the northeastern North Atlantic. The regional model is forced with wind and wave boundary conditions (dynamic downscaling to a spatial resolution of 10–11 km) from the European Centre for Medium-Range Weather Forecasts (ECMWF) ERA-40 reanalysis (from 1958–2002) [17] and the operational ECMWF analysis data (from 2002–2011). Previous analysis on mean wave power variability using the same data had investigated the comparisons of model and buoy data in terms of the annual mean values at Haltenbanken and a location close to Andrew, and in general the agreement is reasonable [12].

The wave data available in 3 h intervals (per sea-state) contain information such as date, time, significant wave height (H_s), peak spectral wave period (T_p), mean wave period (T_m), wind speed, wind and wave directions. We calculate the wave power per unit length of wavefront per sea-state as:

$$P = \frac{\rho g^2}{64\pi} H_s^2 T_e \tag{1}$$

where ρ is the water density, g is the gravitational acceleration and T_e is the energy period, estimated to be midway between T_p and T_m [15]. The average wave power per metre of wavefront for a year (expressed in kW/m) is obtained by numerical integration of the wave power values for all sea-states over that particular year. A year is defined from the middle of July one year to the middle of July the subsequent year, taking the year date from the part of the record up to December. Hence, the continuous wave power record is split from summer to summer to avoid splitting winters when most energy is available.

A comparison between the actual T_e and the estimated $T_e = (T_p + T_z)/2$ at all seven locations has been performed by Bidlot (private communication), and is shown in the Appendix. The agreement between the two quantities in terms of mean value is found to be very good (justifying the use of the estimated T_e for the NORA10 data); the distribution is however slightly skewed towards higher values for the estimated T_e.

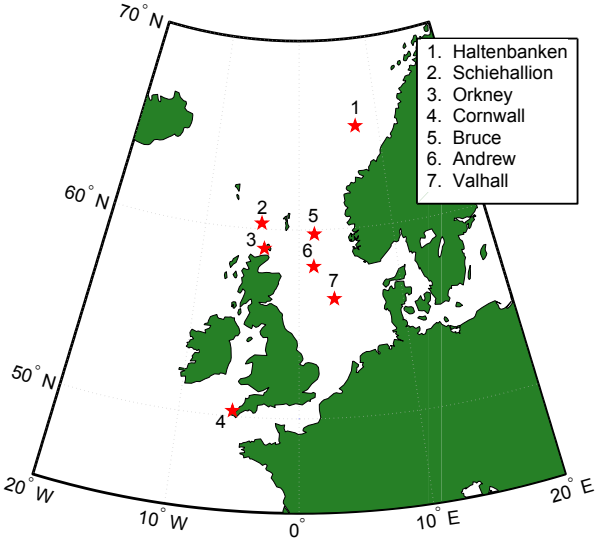

Fig. 1. Map of the locations, with points 1–4 are in the North-East Atlantic, 5–7 in the North Sea.

The practical annual wave power available for conversion at each location can be obtained by incorporating the capture width characteristics of the M4 wave energy converter into the wave power calculation. The M4 machine is a three-float system, each float with a circular cross-section when viewed from above, as shown in Fig. 2. The bow and mid float (float 1 and 2) are rigidly connected, and the larger stern float (float 3) is connected to the mid float by an articulated joint. The power is produced by the relative angular motion of the articulated joint between these two floats. In order to maximise the angular motions of the joint and hence the power take-off, the spacing between each float is kept at about half a wavelength at the optimal operating condition; so the machine fits within a wavelength. For details of the design principles of the M4 machine, see [14].

In this study, we use the rounded end geometry for the M4 machine shown in Fig. 2. Experiments have been conducted by [13] to look at the system response in both regular and irregular waves, and the associated coupled hydrodynamic-structural modelling have been performed by [3] using a dynamic substructuring method. Although an early version of the M4 machine had flat ends to the floats, this produced considerable nonlinear viscous losses, modelled by statistical linearisation in the analysis. In contrast, floats with rounded ends minimise these losses. Comparison of predictions with experimental results, as shown in Fig. 2, suggests that the viscous losses are sufficiently small that they can be ignored. Hence, this study makes use of the simple linear transform function between wave and rotation.

The capture width is defined as the ratio of the average generated power to the ocean wave power resource per unit length of wavefront as defined in Eq. (1). The capture width ratio is then defined as the capture width divided by a wavelength. The comparison in terms of capture width ratio between the experimental results and the numerical modelling for power take-off coefficient (PTO) of 3 Nms (at model scale) is satisfactory, as shown in Fig. 3. Note that there is a slight difference in the quoted experimental results (c.f. Fig. 3 of [13] due to different methods of estimating the ocean wave power resource for irregular waves. The JONSWAP spectral shape is assumed for all sea-states, with γ=3.3 for the peak enhancement factor. T_{r3} is the resonant heave period of the stern float (float 3), a key parameter for sizing the M4 wave energy converter. It is this capture width characteristic that will be used for the power take-off calculations. We take no account of directional spreading in this analysis, simply assuming that the waves are mostly close to uni-directional, while noting that the experiments indicated minimal reduction in directional spread seas, and the M4 machine will generate energy even when aligned along the wave crests (because of the different heave responses of the 3 floats) [3].

The M4 machine is sized based on the long-term average T_e of each location throughout the entire period of the hindcast data. The methodology to obtain the practical annual wave power on a sea-state basis is as follows:

1. Obtain long-term average T_e from the 54 years of hindcast data.
2. Size the machine according to the average T_e, by taking T_{r3} = average T_e.
3. Compute the power on a sea-state basis (H_s, T_e) incorporating the capture width characteristics and assumed mechanical efficiency of 0.9.

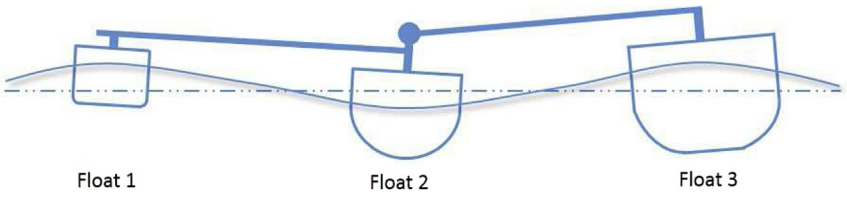

Fig. 2. Sketch showing motions of the M4 machine during the passage of a wave.

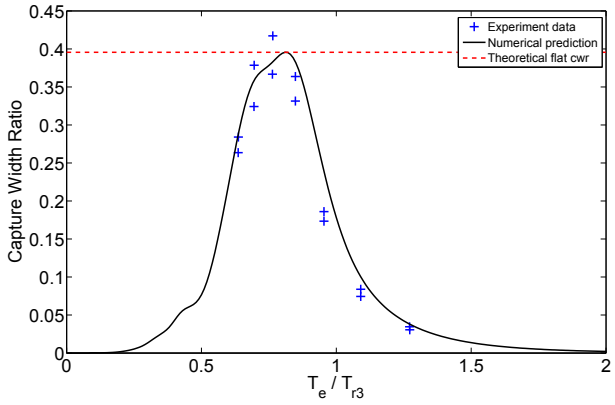

Fig. 3. Variation of capture width ratio with ratio of energy period to resonant heave period of stern float (T_e/T_{r3}) for the M4 wave energy converter for power take-off coefficient (PTO) of 3 Nms (at model scale). Data points are experimental results for uni-directional irregular waves for rounded bases with $\gamma = 3.3$ [13]. For each value of T_e, two values of H_s were tested; the solid line is the numerical prediction from a coupled hydrodynamic-structural model [3], and dashed line is the theoretical flat frequency-independent capture width ratio used for assessment of the ideal practical wave power, where the capture width at the peak is taken as a representative reference.

4. Obtain the average practical power on a year-by-year basis. This is termed the no clipping case.
5. Assume the machine capacity = 3× long-term mean practical power, so power output saturates if the practical power at 3-h interval exceeds this capacity. This is termed the power clipping case.
6. Re-compute the average practical power including clipping until convergence.

Table 1 lists the long-term average T_e for each location. As expected, the locations in the open North Atlantic have the largest average T_e, followed by the locations in the North Sea, which show systematic variation in the north-south direction. Using deepwater wave dispersion theory, the wavelength and hence the machine size scales as period squared. From the seven locations, the ratio of the largest to the smallest M4 machine is close to 2, if the sizing is based on each location. Initially, the analysis will be based on the machine size specific to each location. Subsequently, the sensitivity of the results to machine size will be assessed.

Previous analysis using the same hindcast data has looked at annual mean wave power variability, see [12]. A strong correlation is found between the total annual wave power and the NAO and other atmospheric modes, over some of the locations presented in Fig. 1. In this study, the correlation with the NAO and other atmospheric modes is assessed in terms of the practical annual wave power by including the machine characteristics and clipping criterion.

The NAO is the dominant recurring and persistent large-scale pattern of pressure anomalies (teleconnections) in the North Atlantic. It has long been known to be strongly correlated to the climate variability in the northern hemisphere, particularly in the winter months, see for example [4]. The temporal variability of the NAO and other significant atmospheric modes has been characterised as a set of climate indices. We use monthly climate indices tabulated by National Oceanic and Atmospheric Administration (NOAA) Climate Prediction Center (www.cpc.ncep.noaa.gov) available from January 1950 to the present. For reconstruction of wave power climate back to the past, we include a set of proxy indices derived using the historical reconstructed monthly 500 mbar pressure maps by [5].

We correlate the annual wave power with a winter average of the climate indices, obtained by averaging six month values of monthly indices, defined now as non-dimensional numbers NAO, EA and SCA for the modes described in Section 1, from mid October to mid April. We use a predictor model $P_{predictor}$ for wave power which consists of a linear combination of the climate indices (linear regression), shown as:

$$P_{predictor} = \overline{P} \times \left[1 + b\left(EA_{hi}(t) - \overline{EA}\right) + c\left(NAO(t) - \overline{NAO}\right) + d\left(SCA_{hi}(t) - \overline{SCA}\right)\right] \quad (2)$$

where $P(t)$ is the annual wave power signal, and $\overline{P}$ is the average power over the period of available data. We remove the long time-scale variations in the EA and the SCA as both of them are correlated to the NAO, hence $EA_{hi}(t)$ and $SCA_{hi}(t)$ are the high-pass filtered EA and SCA signals, and $NAO(t)$ is the NAO signal. $\overline{EA}$, $\overline{SCA}$ and $\overline{NAO}$ are the mean of the $EA_{hi}(t)$, $SCA_{hi}(t)$ and $NAO(t)$ signals, respectively. b, c and d are non-dimensionalised constants reflecting the relative importance of the EA, the SCA and the NAO signals in predicting

Table 1
Summary of the results of the ideal practical (flat frequency-independent capture width ratio and no clipping) and practical wave power output (M4 frequency-dependent capture width ratio with power clipping) for all locations. CV is the ratio of standard deviation to mean and R^2 is correlation coefficient.

Location	Average T_e	Ideal practical wave power			Practical wave power			Power output
	(sec)	Mean (kW)	CV	R^2	Mean (kW)	CV	R^2	Efficiency
1. Haltenbanken	8.29	1177	22%	0.71	414	10%	0.58	35%
2. Schiehallion	8.74	1731	19%	0.76	652	8%	0.61	38%
3. Orkney	8.44	937	24%	0.72	319	13%	0.65	34%
4. Cornwall	7.96	455	16%	0.45	147	9%	0.24	32%
5. Bruce	7.59	730	14%	0.62	292	8%	0.56	40%
6. Andrew	6.98	484	14%	0.47	179	8%	0.51	37%
7. Valhall	6.54	339	17%	0.54	116	8%	0.49	34%

wave power, respectively. We train the predictor model by minimising the variance between the wave power from the model and the hindcast over the period of available hindcast data. The individual cut-off values of the high-pass filters and the values of the non-dimensionalised constants are chosen to minimise the variance in each case. For more details of the predictor model, see [12].

3. Power take-off statistics

3.1. Practical annual wave power

Following the methodology presented in Section 2, both the ideal practical and practical annual wave power can be obtained. The practical wave power is obtained by taking the M4 capture width at every wave frequency into the power calculation, while the ideal practical wave power is assessed by incorporating a flat frequency-independent capture width ratio, i.e. by taking the capture width at the peak capture width ratio as a reference into the power calculation for all wave frequencies, see Fig. 2. This capture width represents a physical limit of energy capture for the machine (in terms of length of crest). The ideal practical wave power is useful to define power output efficiency at each location, and also comparing or contrasting the effect of capture width. The ideal practical wave power may also be considered to be an indication of what is possible through reactive control rather than through the simple damping factor of these tests. The feasibility of such control is another important area for investigation.

Fig. 4 shows a comparison of the ideal practical (black lines) and the practical (red lines) annual wave power at Schiehallion. Dashed lines are the wave power with no clipping, solid lines with power clipping. Comparing the two dashed lines shows the important effect of the actual power capture width ratio of the M4 machine. The obvious reductions in the long-term mean power and year-by-year variability are clear. Nevertheless, the temporal variability is quite similar because the M4 capture width characteristics are relatively broad in frequency. Hence, having established a strong association between the ocean wave power resource and the NAO [12], one would also expect a reasonable correlation for the practical wave power produced by the M4 machine. In Section 4, different bandwidths for the capture width ratio are investigated to assess the impact on the produced power.

Also, on Fig. 4, comparing the dashed to the solid lines shows the effect of power clipping. For the flat capture width ratio (giving idealised practical power), the effect is shown to be more important: clipping produces a pronounced reduction in long-term mean and overall variability. The severe reduction for the flat capture width ratio is straightforward to explain as the larger waves are not being fully utilised due to power clipping. Interestingly though, the effect with the actual capture width characteristic of the M4 machine is much less prominent despite the same power clipping criterion. This is probably due to the effect of finite bandwidth and the way the M4 machine is sized, which is based on the long-term average T_e. In Section 4, the effect of power clipping at different levels of output capacity is considered.

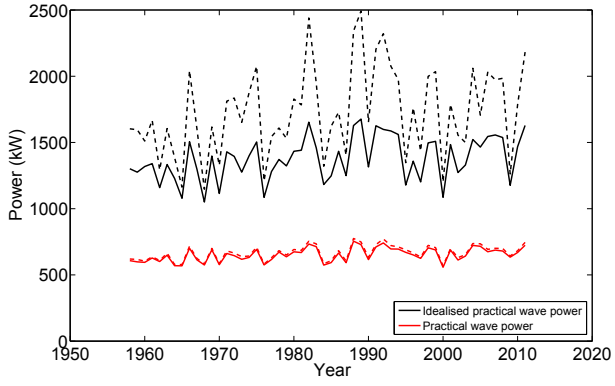

Fig. 4. Annual mean ideal practical and practical wave power comparison at Schiehallion. Dashed lines are the power output without saturation (no clipping), solid lines with saturation (clipped at 3× long-term mean power). Note the red dashed line is almost coincident with the full line. (For interpretation of the references to colour in this figure legend, the reader is referred to the web version of this article.)

Table 1 summarises the results for both the ideal practical (flat capture width ratio and no clipping) and practical wave power (actual machine capture width ratio with power clipping) for each location. The temporal variability is quantified as a coefficient of variation (CV), defined as the ratio of the standard deviation to the mean. The locations in the North Sea are sheltered by surrounding land, hence the long-term mean power and CV are generally smaller than those in the open North Atlantic locations. Also, there are effectively two directionally-opposite sectors of dominant waves leading to reduced variability in the available wave power in the North Sea as opposed to a single dominant directional sector in the open North Atlantic [12]. The power efficiency, defined as the ratio of practical wave power to idealised practical wave power, seems to be comparable for all locations.

It is worth noting that the long-term average T_e alone is not a direct measure of wave severity or power output. For instance, Cornwall, despite having larger average T_e than Bruce or Andrew and hence larger machine size, produces smaller power output as the waves are smaller in magnitude. Thus, sizing the M4 machine based on the average T_e might not be optimum with Cornwall for example. This is discussed further in Section 4, where the effect of altering the machine size is investigated.

Fig. 5 shows the temporal variation of the practical wave power (solid lines) for: (a) the open North Atlantic locations, and (b) the North Sea locations. It can be observed that there are similar interannual and decadal structures among the locations in the open North Atlantic (except Cornwall), and among the locations in the North Sea. Between the two groups of locations, the temporal structures are also quite similar. Cornwall is different perhaps because of the close proximity to the coast and a relatively distant sheltering effect by Ireland.

3.2. Correlation with the teleconnections

The ocean wave power resource in the North-East Atlantic and North Sea has been shown to be strongly influenced by the natural variability [12]. If the practical wave power is also strongly influenced, forecasting the wave power output over long times might be a challenging task. Here we use the predictor model as described in Section 2 to investigate the correlation.

The correlation results are shown in Fig. 5 as dashed lines together with the R^2 values. Table 1 shows the summary of the R^2 values for both the ideal practical and practical mean wave power for each location. In general, the strength of the correlation decreases from the ideal to the practical wave power, demonstrating the effect of capture width in weakening the correlation to the climate variability. However, the correlation is still reasonably high for all locations except Cornwall. At least half of the longer-than-annual variability of the practical wave power signal is explained by the variability of the NAO and other atmospheric modes.

Orkney, a location close to EMEC testing site, has the highest R^2 value ($R^2 = 0.65$) and also the largest variability (CV = 13%) among all the locations. This leads us to perform a reconstruction of practical wave power output at Orkney from 1665–2005. For such, we use the same proxy climate indices from 1659–1998 as used previously in [12]; and the climate indices from the Climate

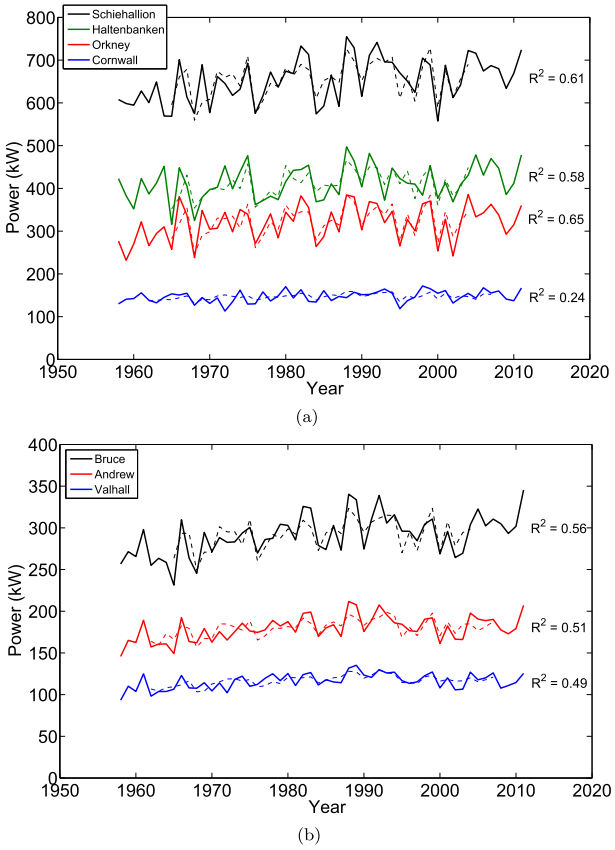

Fig. 5. Annual mean M4 wave power output (solid lines) and the teleconnection-based predictions (dashed lines) at all locations. (a) For the open North Atlantic locations. (b) For the North Sea locations.

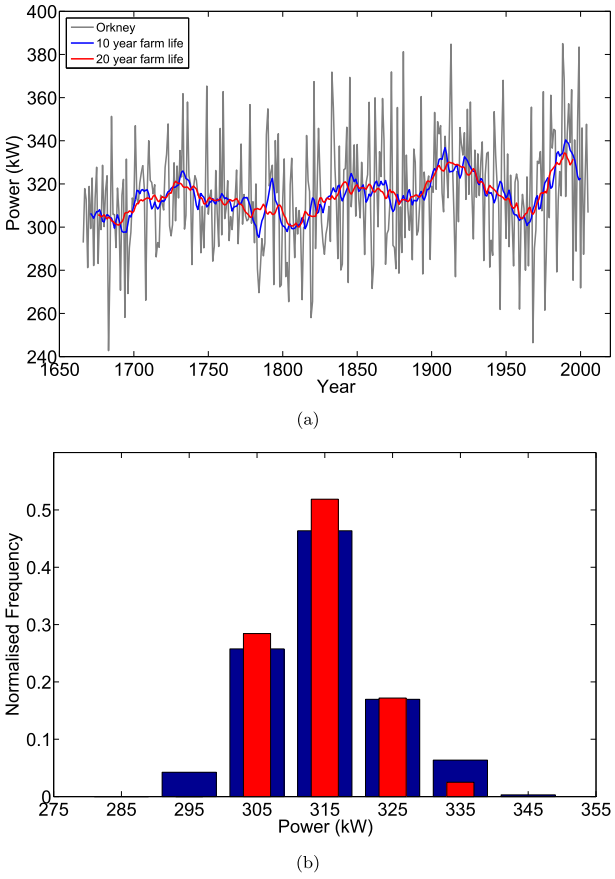

Fig. 6. Reconstructed practical wave power output at Orkney from 1665–2005. (a) In terms of temporal variation of the power output (grey), also shown is the 10 (blue) and 20 year (red) moving average lines representing the average practical power output over the intended operational life of the M4 farm. (b) In terms of histograms of the frequency of occurrence of the average power over 10 and 20 years of farm life. (For interpretation of the references to colour in this figure legend, the reader is referred to the web version of this article.)

Prediction Center (CPC) from 1998–2005. The proxy indices are obtained by regressing the climate indices with the historical reconstructed monthly 500 mbar pressure maps computed by [5]; over the overlapping period from 1950–1998, and averaging the pressure-time histories over the regions of high correlation from 1665–1998 to produce the proxy indices. For more details of the proxy indices, see [12].

Fig. 6(a) shows the estimated historic practical wave power at Orkney. Interannual and multidecadal variability on all timescales is apparent, with the highest and lowest power being ±20% of the mean over the entire reconstruction. This level of total variability, fortunately, is much smaller than that of the ocean wave power resource, as reported in [12]. Thus, with the inclusion of the realistic M4 capture width characteristics, much of the variability in the practical wave power gets smeared out despite the positive correlation with the NAO.

To assess the long-term economic viability of the M4 machine, 10 and 20 year moving averages are added to obtain the average practical wave power output over a realistic intended operational life of a farm. The interannual variability has been smeared out leaving only the long-term multidecadal fluctuation. The largest variability is seen during the period from 1960s to 1990s: a 10% difference in the power output. This level of uncertainty should be considered in any long-term reliability analysis and in power scheme economics for the M4 wave energy converter.

As the practical wave power at Orkney is influenced by the natural variability to some extent, forecasting the power output will mostly depend on how the NAO and other modes will behave. Nevertheless, the reconstruction analysis provides a useful guidance over the practical range of the power output produced in the past. Fig. 6(b) shows the histograms of the frequency of occurrence of the average power produced over the intended operational life of 10 and 20 years. The shape of the histograms is approximately normally distributed, with the most likely production at about 315 kW for the M4 machine sized specific to that location, and a long-term possible variation of ±10–15% over the assumed life of the farm.

4. Sensitivity studies

Having looked at the practical wave power and established positive correlation with the NAO, we are interested to explore how sensitive the wave power output is to some key parameters for the M4 machine. It is interesting to investigate whether changing one of the pertinent parameters will reduce or amplify any influence of the climate variability.

4.1. Size of machine

It is important to investigate the effect of machine size for all the locations shown in Fig. 1. For that, first, we look at the size of machine specific to each location and linearly scale the machine dimensions, so that 1× corresponds to the design criteria presented in Section 2. Subsequently, we define three sizes for all locations, and investigate the behaviour of the practical power output at each location with respect to the three sizes.

Fig. 7(a) shows the variation of the practical long-term mean wave power output with respect to linear scaling of the original

machine. The long-term mean power at each location scales as the severity of the sea-state. It is obvious that the long-term mean power (likewise the variability) increases as the relative machine size is increased, reaching a maximum value at about 2–2.2× the original size. Thus, if the aim is to produce as much power as possible with a single machine, one simply has to scale the machine size up. However, the variation of the power to the machine size is nonlinear around the peak value, which means there will be a difference in the economic cost of having a single larger machine compared to several smaller machines.

By normalising the mean power output by the value at the original size for each location and plotting the vertical axis in a logarithmic scale, a reasonable collapse in the variation of the power output for all locations is obtained, as shown in Fig. 7(b). This demonstrates that the performance of the M4 machine in terms of different sizing is universal regardless of the locations or different sea-states, which is an interesting and useful observation.

Cost might be thought to be proportional to mass or length^3. However, cost of steel is an important driver and steel thickness is typically 10 mm for ships or offshore structures of this size. Since ballast is of low cost, this would suggest cost proportional to length^2. However, other costs, e.g. the PTO and mooring, are likely to increase with mass and hence a power somewhere between 2 and 3 is likely. Thus we investigate sensitivities to powers of 2, 2.5 and 3.

To illustrate the difference in the economic cost, the normalised mean power output for each location is plotted against cost ratio in a logarithmic scale, as shown in Fig. 7(c). The cost ratio is defined as the cost for linear scaling of the original machine relative to the original cost. Three different variations of cost as a function of size result in three bands of normalised power output. Also shown in the plot is the variation of normalised power output with the cost ratio of simply having more machines of the original size (power ~ cost, dashed line), with open circles representing integer numbers of the multiple machines. For a given economic cost, it is observed that the power produced by multiple units of original sized machine is higher than by a single unit of larger size. Hence, ignoring survivability criteria, it appears that having multiple units of the original sized machine is a better option than having a single unit of larger size. When assessing survivability in extreme storms, a different conclusion may emerge. This will be investigated in future work.

Sizing each machine specific to each location may not be economically optimum for mass production of the M4 wave energy converter. Perhaps, one or two different sizes of the M4 machine could be deployed throughout the entire UK waters. To investigate the optimum machine size, three different sizes fixed at $T_{r3} = 6.5$, 7.5 and 8.5 s are assessed over the entire locations (termed small, medium and large, respectively), and the variation of the mean wave power with machine size can be obtained.

Fig. 8 shows the variation of long-term mean power relative to that of a small machine with the three machine sizes for all locations (solid lines). Also shown are the three different variations of cost relative to the cost of having a small machine (dashed lines) as a function of length (and period). The variation for Schiehallion, Haltenbanken and Orkney have steeper slopes than cost ~ length$^{2.5}$ line, while for the rest of the locations the slope are in between cost ~ length$^{2.5}$ and length^2 lines. If the cost of one M4 machine is proportional to length$^{2.5}$, which is perhaps more likely than length^2 and length^3, the analysis seems to suggest that the size does not

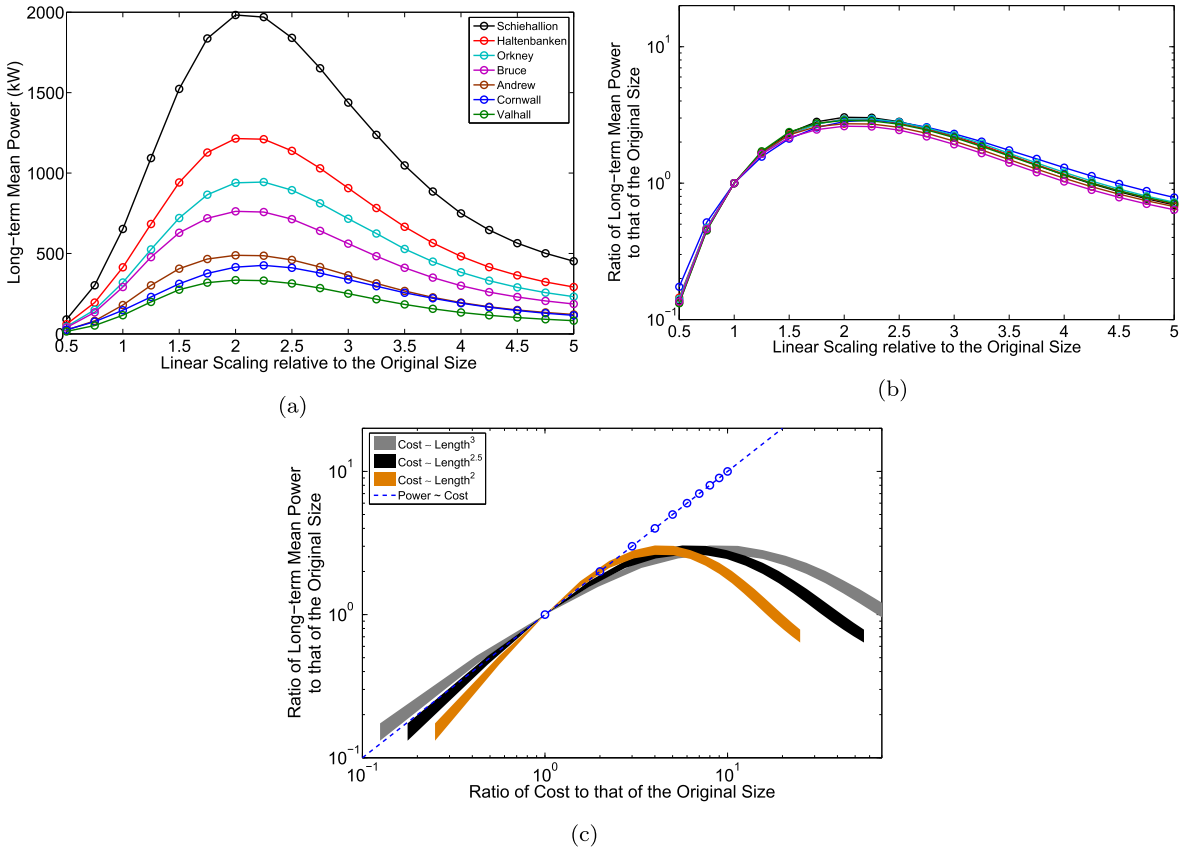

Fig. 7. (a) and (b) Variation of the long-term mean practical wave power output with linear scaling of the original machine. (a) In terms of absolute power output value. (b) In terms of normalised power output to the value at the original size. (c) Variation of three bands of normalised power output with cost ratio, assuming three variations of cost as a function of size. Also shown is the variation of normalised power output with the cost ratio of having more machines of the original size. Open circles denote integer numbers of the multiple machines.

matter for the open North Atlantic locations (Schiehallion, Haltenbanken and Orkney): the size is simply proportional to the power output. For the North Sea locations and Cornwall, it is likely that small to medium size is more economically viable than a large size. Hence, two different sizes might be optimum for all locations: a large machine for the open North Atlantic locations ($T_{r3} = 8.5$ sec), and a small machine for the North Sea locations and Cornwall ($T_{r3} = 6.5$ sec). In particular, Cornwall is better suited to a smaller machine than the original size ($T_{r3} = 7.96$ sec) which is based on the long-term average T_e at that location. However, the correlation for Cornwall is substantially weaker so we have much less confidence in our long-term power prediction.

4.2. Effect of power clipping

Here, we investigate the effect of clipping the wave power at different levels of output capacity. The original design format introduced in Section 2 is to set the capacity at 3× long-term mean power, so the power output simply saturates if the computed power at any 3-h interval exceeds this capacity. Fig. 9 shows the variation of the practical wave power output at Schiehallion for different capacity set at 2×, 3× and 4× long-term mean power (solid lines). Also shown is the power output with no clipping (dashed line).

Taking the no clipping case as the benchmark, it is apparent that clipping at 4× long-term mean power has negligible effect on the structure of the power output. Clipping at 3×, as shown previously in Section 3.1, introduces a small change in the long-term mean value (a 2% reduction). In contrast, clipping at 2× reduces the long-term mean value by 15% as well as reducing the temporal variability, although the variation of this over time is very similar to clipping at 3×. The further reduction is consistent as more large waves are not well exploited with this more stringent limitation. Thus, clipping at 3× long-term mean power seems to be a good choice, at least for the M4 capture width characteristics.

4.3. Effect of power take-off system

Here, we look at the changes in the wave power output due to different settings for the damping or power take-off coefficient (PTO), where the system is represented by a linear damper in [3]. Fig. 10 shows the variation of the capture width ratio for different settings for the PTO coefficient (at model scale). It can be seen that there is more variation in the vertical direction than in the horizontal direction (bandwidth of the capture width ratio).

Fig. 11 shows the resultant variation of practical wave power output due to different settings for the PTO with standard 3× mean power clipping at Orkney. As expected, the long-term mean power

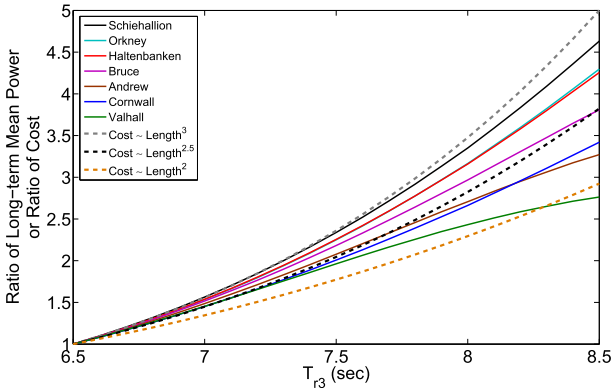

Fig. 8. Variation of long-term mean wave power output and cost relative to those of a small machine ($T_r = 6.5$ sec) with the three machine sizes.

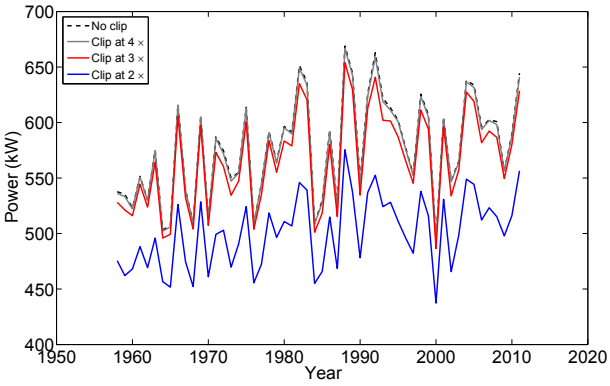

Fig. 9. Variation of the practical wave power output with different clipping for Schiehallion.

varies with the PTO coefficient, with an optimum PTO coefficient of 3 Nms, which is the base case. Unlike the case of the power clipping sensitivity study, the interannual and decadal variability is essentially unaffected for the different PTO coefficients considered, and this holds for all locations. This is presumably because there is little change in the bandwidth of the capture width ratio for different settings for the PTO coefficient. The effect of perturbing the power absorption bandwidth is considered next.

4.4. Effect of the bandwidth of the capture width characteristics

To perturb the bandwidth of the capture width characteristics, two cases are considered: broadening (1.5×) and narrowing (0.75×) the bandwidth relative to capture width ratio for PTO = 3 Nms, which is the base case. The increased bandwidth with the same peak capture width ratio may be produced by reactive control of the PTO which would be an important area for further investigation. Reduced bandwidth and peak capture width ratio may be caused by malfunction or by a PTO in need of service.

Fig. 12 shows the variation of the capture width ratio for the two cases in addition to the base case. The bandwidth is adjusted gradually to allow for smooth variation with the period ratio at the peak value being fixed. For the broadening case, the asymptotic limit is similar to the theoretical flat frequency-independent capture width ratio as described previously in Section 3.1, but with more weighting towards larger waves with longer periods (where here $P \propto T_e^3$ following deepwater wave dispersion theory instead of $P \propto T_e$ as defined in Eq. (1) and used in Section 3.1) which will give rise to a difference in the temporal variation of wave power. For the

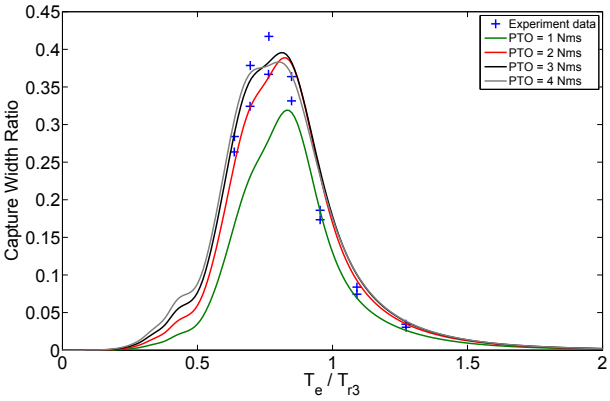

Fig. 10. Variation of capture width ratio with ratio of energy period to resonant heave period on stern float (T_e/T_{r3}) for different power take-off coefficients (PTO). PTO coefficient of 3 Nms (at model scale) is the base case.

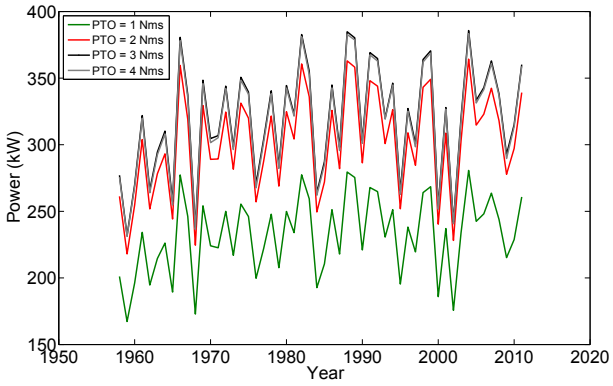

Fig. 11. Variation of practical wave power output at Orkney for different power take-off coefficients (PTO) with power clipping. PTO coefficient of 3 Nms (at model scale) is the base case.

narrowing case, the frequency variation in the capture width more closely resembles that for a single point absorber.

Fig. 13 shows the effect of the bandwidth on the practical wave power output with standard 3× mean power clipping at Orkney. It is evident that as the bandwidth gets broader, both the long-term mean and the variability are increased, and vice versa when the bandwidth is reduced. In general, the correlation with the NAO increases with broader bandwidth. Having broader capture width characteristics is perhaps desirable as the long-term mean power is higher. However, this has to be balanced by the amount of fluctuation in power output caused by the climate variability, especially for the locations in the open North Atlantic.

5. Conclusions

The practical wave power produced by the M4 machine is variable over annual and decadal timescales, particularly in the open North Atlantic. This temporal structure is somewhat comparable to the variation in the ocean wave power resource, due to the M4 capture width characteristics being relatively broadband. As a result, the produced wave power is influenced by the climate variability to some extent, but at a reduced degree of variability compared to the ocean wave power resource. In this study, we establish the NAO as the dominant physical mechanism driving the longer-than-annual power variability produced by the M4 machine.

Sensitivity studies have been conducted to assess the importance of some key design parameters for the M4 machine, which are helpful for long-term power scheme economics. The M4

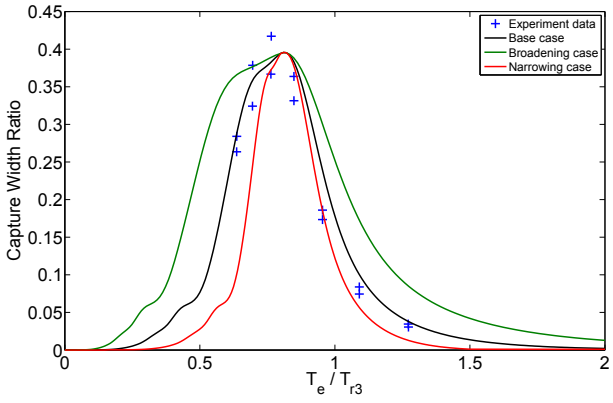

Fig. 12. Variation of capture width ratio with ratio of energy period to resonant heave period on stern float (T_e/T_{r3}) for different bandwidths.

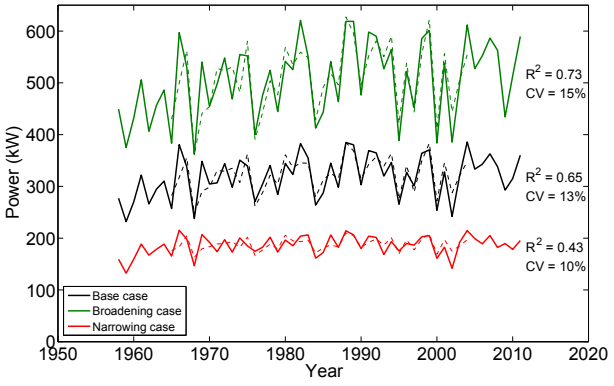

Fig. 13. Variation of practical wave power output at Orkney for different bandwidths with power clipping.

concept is promising because:

- the performance of the M4 machine scaled linearly relative to the original size is independent of the locations or the sea-states,
- ignoring survivability criteria, multiple original sized machines are more economically viable than fewer larger ones,
- for mass production of the M4 machine, two different sizes are optimum for all locations: a large machine for the open North Atlantic locations and a smaller machine for the North Sea locations and Cornwall,
- clipping at ≥3× long-term mean power does not affect the temporal structure of the power output significantly,
- the correlations with the NAO and other atmospheric modes work reasonably well for most of the locations except Cornwall, and are slightly weakened by non-linearity in clipping and more narrow banded responses possible with control,
- broader capture width characteristics produce higher long-term mean power, however at the expense of increased temporal variability driven primarily by the NAO.

To utilise the predictability of the M4 wave power production in the North-East Atlantic and the North Sea, we realise that the ability to forecast the NAO into the future remains essential. However, with a reconstruction of practical wave power output, we are able to estimate the possible range of variability to be experienced over decadal timescales. This paper clearly shows that the large-scale geophysical processes in the eastern North Atlantic, the North Atlantic Oscillation with the East Atlantic and the Scandinavian patterns, should be taken into account when assessing the viability of wave power schemes. This study is not only relevant to the M4 machine, but because of the implications, the statistical approach used here is potentially relevant to other wave energy converters as well.

Acknowledgements

We thank Dr. Richard Gibson now at Offshore Consulting Group and BP Sunbury for providing the wave data and acknowledge support from EPSRC (project EP/J010316/1 Supergen MARine TechnologY challenge and project EP/K012487/1 Supergen Marine Challenge 2 Step-WEC). We are grateful to Dr. Jean Bidlot of ECMWF for providing the comparison shown in Fig. 14.

Appendix

A comparison between the actual T_e and the estimated $T_e = (T_p + T_z)/2$ at all seven locations (Bidlot, private communication) is shown in Fig. 14. This was performed by using a recent 36 year

hindcast of the latest operational model version (ECWAM) forced by ERA-interim data.

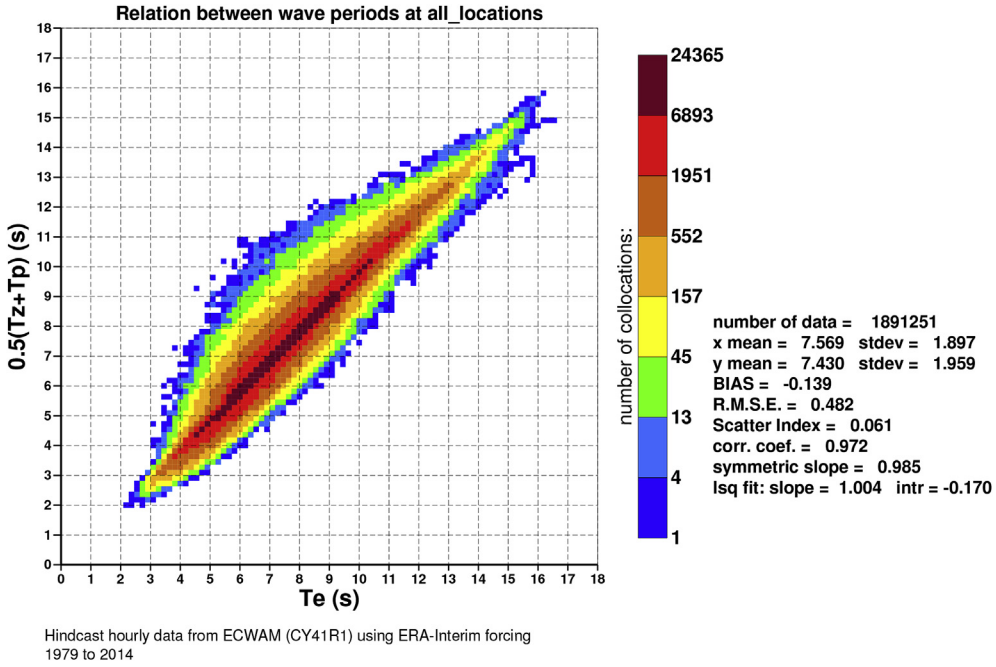

Fig. 14. Comparison between the actual T_e and the estimated T_e at all locations provided by [1].

References

[1] J. Bidlot, Hindcast Hourly Data from ECWAM (CY41R1) Using ERA-interim Forcing from 1979 to 2014 (Private communication), 2016.

[2] P.D. Bromirski, D.R. Cayan, Wave power variability and trends across the North Atlantic influenced by decadal climate patterns, J. Geophys. Res. Oceans 120 (5) (2015) 3419–3443.

[3] R. Eatock Taylor, P.H. Taylor, P.K. Stansby, A coupled hydrodynamic-structural model of the M4 wave energy converter, J. Fluids Struct. (2015) (under review).

[4] J.W. Hurrell, Y. Kushnir, G. Ottersen, M. Visbeck, An Overview of the North Atlantic Oscillation, American Geophysical Union, 2003.

[5] J. Luterbacher, E. Xoplaki, D. Dietrich, R. Rickli, J. Jacobeit, C. Beck, D. Gyalistras, C. Schmutz, H. Wanner, Reconstruction of sea level pressure fields over the Eastern North Atlantic and Europe back to 1500, Clim. Dyn. 18 (7) (2002) 545–561.

[6] E.B. Mackay, A.S. Bahaj, P.G. Challenor, Uncertainty in wave energy resource assessment. Part 2: variability and predictability, Renew. Energy 35 (8) (2010) 1809–1819.

[7] S.P. Neill, M.R. Hashemi, Wave power variability over the northwest European shelf seas, Appl. Energy 106 (2013) 31–46.

[8] S.P. Neill, M.J. Lewis, M.R. Hashemi, E. Slater, J. Lawrence, S.A. Spall, Inter-annual and inter-seasonal variability of the Orkney wave power resource, Appl. Energy 132 (2014) 339–348.

[9] B. Reguero, I. Losada, F. Méndez, A global wave power resource and its seasonal, interannual and long-term variability, Appl. Energy 148 (2015) 366–380.

[10] M. Reistad, Ø. Breivik, H. Haakenstad, O.J. Aarnes, B.R. Furevik, J.-R. Bidlot, A high-resolution hindcast of wind and waves for the North Sea, the Norwegian Sea, and the Barents Sea, J. Geophys. Res. Oceans (1978–2012) 116 (C5) (2011).

[11] H. Santo, P.H. Taylor, T. Woollings, R. Gibson, Decadal variability of extreme wave heights as a measure of storm severity in the North-East Atlantic and North Sea, Geophys. Res. Lett. (2015a) (under review).

[12] H. Santo, P.H. Taylor, T. Woollings, S. Poulson, Decadal wave power variability in the North-East Atlantic and North Sea, Geophys. Res. Lett. 42 (12) (2015b) 4956–4963.

[13] P. Stansby, E.C. Moreno, T. Stallard, Capture width of the three-float multi-mode multi-resonance broadband wave energy line absorber M4 from laboratory studies with irregular waves of different spectral shape and directional spread, J. Ocean Eng. Mar. Energy (2015a) 1–12.

[14] P. Stansby, E.C. Moreno, T. Stallard, A. Maggi, Three-float broad-band resonant line absorber with surge for wave energy conversion, Renew. Energy 78 (2015b) 132–140.

[15] M.J. Tucker, E.G. Pitt, Waves in Ocean Engineering, vol. 5, Elsevier, 2001.

[16] P. Unden, L. Rontu, H. Järvinen, P. Lynch, J. Calvo, G. Cats, J. Cuxart, K. Eerola, C. Fortelius, J.A. Garcia-Moya, et al., HIRLAM-5 Scientific Documentation, 2002.

[17] S.M. Uppala, P. Kållberg, A. Simmons, U. Andrae, V. Bechtold, M. Fiorino, J. Gibson, J. Haseler, A. Hernandez, G. Kelly, et al., The ERA-40 re-analysis, Q. J. R. Meteorological Soc. 131 (612) (2005) 2961–3012.

[18] T. WAMDI Group, The WAM model-a third generation ocean wave prediction model, J. Phys. Oceanogr. 18 (12) (1988) 1775–1810.